NANO LETTERS

2008
Vol. 8, No. 1
310−316

Single Particle X-ray Diffractive Imaging

Michael J. Bogan,*,† W. Henry Benner,† Sébastien Boutet,†,‡,§ Urs Rohner,† Matthias Frank,† Anton Barty,† M. Marvin Seibert,§ Filipe Maia,§ Stefano Marchesini,†,# Saša Bajt,†,+ Bruce Woods,† Vincent Riot,† Stefan P. Hau-Riege,† Martin Svenda,§ Erik Marklund,§ Eberhard Spiller,|| Janos Hajdu,‡,§ and Henry N. Chapman†,⊥

Lawrence Livermore National Laboratory, 7000 East Avenue, Livermore, California 94550, Stanford Synchrotron Radiation Laboratory, Stanford Linear Accelerator Center, 2575 Sand Hill Road, Menlo Park, California 94305, Laboratory of Molecular Biophysics, Institute of Cell and Molecular Biology, Uppsala University, Husargatan 3, Box 596, S-75124 Uppsala, Sweden, Spiller X-ray Optics, Livermore, California 94550, and Centre for Free-Electron Laser Science, Universität Hamburg, Notkestraβe 85, 22607 Hamburg, Germany

Received October 22, 2007; Revised Manuscript Received November 28, 2007

ABSTRACT

In nanotechnology, strategies for the creation and manipulation of nanoparticles in the gas phase are critically important for surface modification and substrate-free characterization. Recent coherent diffractive imaging with intense femtosecond X-ray pulses has verified the capability of single-shot imaging of nanoscale objects at suboptical resolutions beyond the radiation-induced damage threshold. By intercepting electrospray-generated particles with a single 15 femtosecond soft-X-ray pulse, we demonstrate diffractive imaging of a nanoscale specimen in free flight for the first time, an important step toward imaging uncrystallized biomolecules.

Development of methods enabling higher spatial and time resolution characterization of nanoscale objects such as single particles and biomolecules is essential to achieve the goals of nanotechnology and to push structural biology into new frontiers. We are developing strategies to enable characterization of nanoscale objects using the first operational soft X-ray free electron laser (FEL), the FLASH facility at DESY in Hamburg, Germany.[1,2] This facility produces ultrafast (<30 fs) and ultrabright coherent X-ray pulses (peak brightness $>10^{30}$ photons/s/mrad^2/mm^2 /(0.1% bandwith) or $>10^{12}$ photons/pulse) and provides many new possibilities for probing nanoscale objects.[3] Examples of new capabilities demonstrated at FLASH include femtosecond time-resolved holography for measurements of nanoparticle dynamics[4] and single-pulse diffractive imaging of nanostructured materials.[5] In diffractive imaging, a sample is illuminated by coherent X-rays, a far-field diffraction pattern is recorded on an area detector, such as a charge-coupled device (CCD), and the image is reconstructed using iterative phase retrieval algorithms.[6,7] During initial experiments at FLASH, samples were mounted on supporting silicon nitride membranes that contributed background scattering to the measurements. When the number of atoms in the substrate becomes much larger than the number of atoms in the sample itself, such as in the case of isolated biomolecules on a membrane, this background is expected to dominate the signal measured by the CCD. This motivates the development of sample handling systems free of supporting membranes, such as particle beams, for introducing particles and biomolecules into the X-ray beam. Successful implementation of such container-free sampling methods may enable structural determinations without the need for a crystal.[8−10]

Particle beams have been at the vanguard of research in most branches of science. Recently, strategies for manipulating nanoparticles in the gas phase using their inertial properties are gaining interest in the manufacture of nanostructured materials[11,12] and for substrate-free particle characterization in vacuo.[13−15] A key development in the generation of focused nanoparticle beams in vacuo was Liu et al.'s implementation of thin plate orifices to manipulate particle spatial distribution prior to them passing through a nozzle and subsequently undergoing supersonic expan-

* Corresponding author. E-mail: bogan2@llnl.gov.
† Lawrence Livermore National Laboratory.
‡ Stanford Linear Accelerator Center.
§ Uppsala University.
|| Spiller X-ray Optics.
⊥ Universität Hamburg.
Current Address: Advanced Light Source, MS 2-400, Lawrence Berkeley National Laboratory, 1 Cyclotron Road, Berkeley, CA 94720, USA.
+ Current Address: Deutches Elektronen Synchrotron, Notkestraβe 85, 22607 Hamburg, Germany.

10.1021/nl072728k CCC: $40.75
Published on Web 12/21/2007

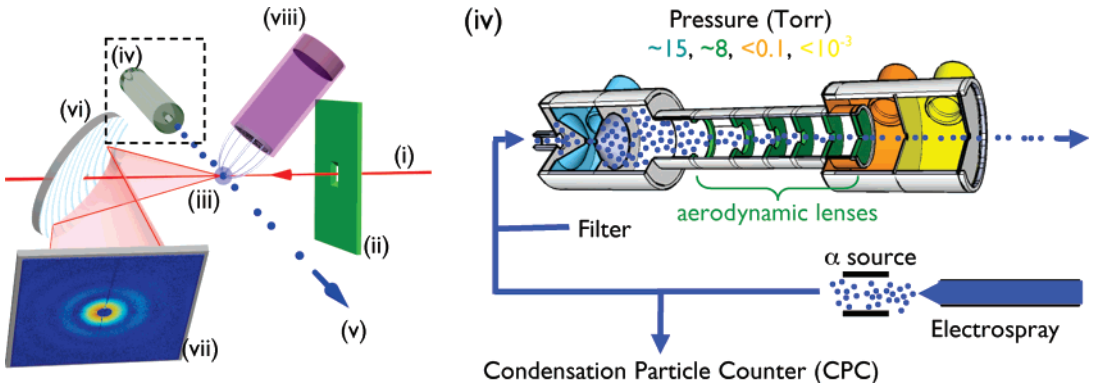

Figure 1. Schematic diagram of the experimental apparatus (not to scale). The FEL pulses (i) are incident from the right, pass through an aperture designed to block stray light (ii), and are focused to a 20 μm spot that defines the interaction region (iii). Electrospray-generated aerosol is charge-neutralized via an α-source and delivered into vacuum through a differential pumping interface equipped with an aerodynamic focusing system (iv). The pressure in the three pumping regions, colored blue, orange, and yellow, is set to optimize the focusing of the nanoparticles through an aerodynamic lens stack (green). The resultant continuous stream of nanoparticles travels at ~150 m/s and is confined to a beam of ~250 μm diameter (v). The nanoparticles are steered into the interaction region using mechanical translation of the entire differential pumping interface. X-rays diffracted from the interception of single nanoparticles by the FEL reflect from a graded multilayer planar mirror (vi) to the single photon sensitive X-ray CCD (vii) while the direct beam passes through a hole in the center of the mirror. Ions created from the FEL interactions are detected by a miniature TOFMS (viii).

sion.[16,17] An axisymmetric stack of these thin plate orifices, or aerodynamic lenses, provides successive contractions of a flowing particle beam and enables focusing of a wide range of particle sizes (1 nm to 10 μm).[18] In this letter we demonstrate a viable technique, based on such an aerodynamic lens stack, for introducing isolated single particles in free flight into a pulsed X-ray beam for substrate-free imaging. We demonstrate an imaging resolution of better than 40 nm by diffractive imaging with the single X-ray pulse and further characterize the interaction by mass spectrometry.

Substrate-Free Particle Delivery to X-rays. Our experimental geometry (Figure 1) is based on that previously used to image samples on silicon nitride foils.[5] Pulses from the FLASH FEL are condensed to a 20 μm diameter beam at the sample plane using a grazing-incidence ellipsoidal mirror. No monochromator or pinhole is used to limit the beam, because the FEL output has sufficient temporal and spatial coherence for diffractive imaging. Instead of micropositioning a substrate-supported sample into the beam, the apparatus is designed to introduce a continuous particle beam transmitted by an aerodynamic lens stack into the FEL beam. To steer the particle beam to intersect with the X-ray beam, the aerodynamic lens stack is mechanically translated. This is achieved by translating the entire differential pumping interface, represented in Figure 1 (iv), in which the lens stack is integrated.

The sample is generated using a charge-reduced nanoelectrospray aerosol source.[19] The method is well characterized, has previously been used to prepare samples of spherical nanoparticles on silicon nitride foils for characterization at FLASH,[20] and is applicable to a wide variety of nanoscale materials that are likely to be characterized using FELs including carbon nanotubes,[21] large biomolecules,[22] viruses,[23−25] and cells.[26] One particular sample of interest is scaffolded DNA origami, consisting of double-stranded DNA programmed to form predefined two-dimensional geometrical shapes.[27] We are investigating DNA nanostructures, because

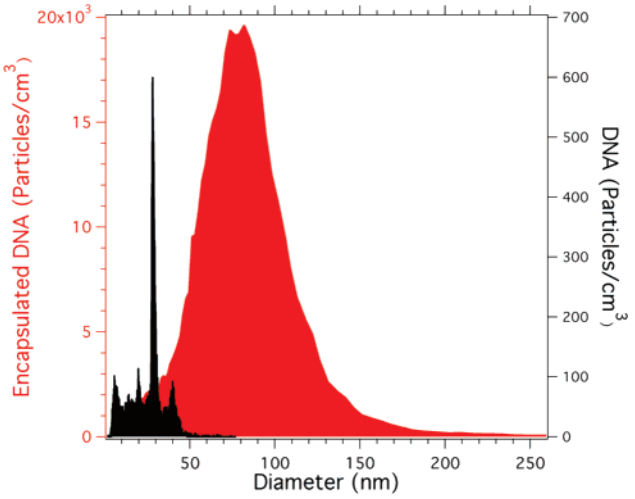

Figure 2. Size distribution of scaffolded DNA electrosprayed from a 25 mM ammonium acetate solution containing 0% (black) and 50% (red) sucrose, as measured by scanning mobility particle size spectrometry. Both bare DNA and sucrose-encapsulated DNA were injected into the FEL beam.

they may be useful as nanobreadboards for the arrangement of nano-objects or biomolecules for enhancing the signal-to-noise ratio in single particle imaging methods, including holography with a complicated reference.[28]

For the first experiments, it was essential to use particles that would produce strong diffraction patterns. When electrosprayed, individual megadalton DNA complexes have an aerodynamic diameter of 28 nm (Figure 2). The X-ray intensity produced by focusing the beam to a diameter of 20 μm was not sufficient to record single pulse diffraction patterns of these particles. We increased the signal by enlarging the particles to increase their scattering cross section. Larger particles were created using Kaufman's in situ electrospray method for synthesis of sucrose-encapsulated biomolecules.[29] Sucrose is added to the starting solution, and upon evaporation of the dilute ammonium acetate/water

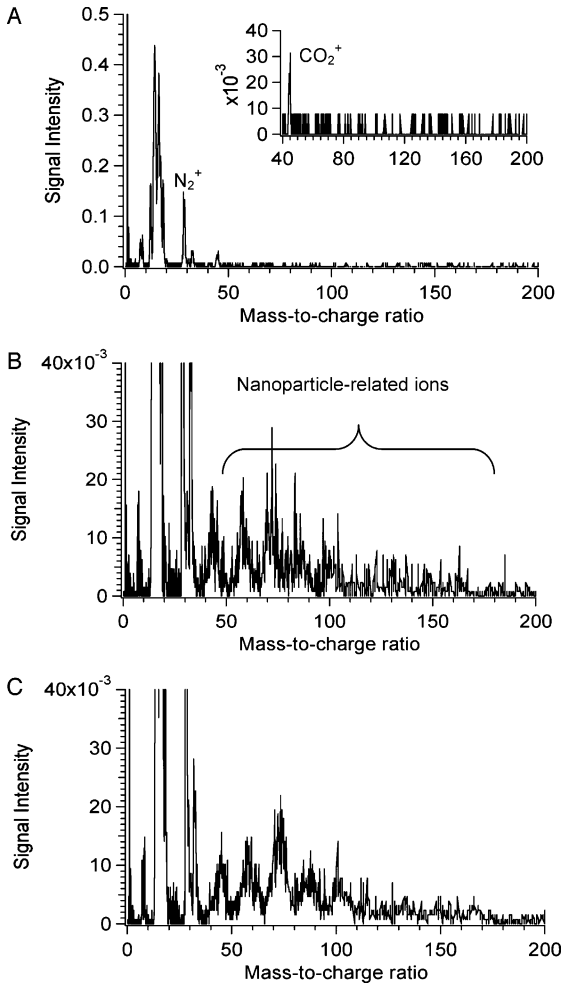

Figure 3. TOFMS of ions created by a single FEL pulse from (A) background gas, (B) the single particle hit in Figure 4 panel A, and (C) the particles hit in Figure 4 panel B.

buffer sucrose-encapsulated DNA is created. The diameter of the composite nanoparticle is given by $[d_m^3 + d_{suc}^3]^{1/3}$, where d_m and d_{suc} are the diameters of the discrete macromolecule (28 nm for the DNA complexes) and residue particles of sucrose (80 nm) when electrosprayed separately.[29] The composite sucrose/DNA particles averaged 81 nm in diameter, and their mass is dominated by the sucrose (Figure 2). Particles larger or smaller than 81 nm resulted from variations in the initial volume of droplets emitted and from periodic instability of the electrospray source. All particle sizes are directed toward the FEL.

Mass Spectrometry. Individual particles are intercepted by the FEL randomly, therefore a time-of-flight mass spectrometer (TOFMS) is used to identify particle interception events. Mass spectra can be collected at a rate of 100 kHz. Gases delivered through the injector to the interaction region (primarily N_2, O_2, and CO_2) were ionized by the FEL, resulting in TOFMS detection of the ions N^{2+}, N^+, O^{2+}, O^+, OH^+, H_2O^+, N_2^+, O_2^+, and CO_2^+ (Figure 3A). Particle interception events produced ions with mass-to-charge ratios greater than 50 (Figure 3B). These ions are consistent with the ions created from sucrose particles in other high-temperature ion sources, such as inductively coupled plasma (7000 K).[30] In this case, the particle is heated to ~60 000 K during the interaction,[5] and the mechanism of ion generation has not been elucidated. These are the first mass spectra ever collected from biological materials ionized by a soft X-ray FEL.

Single Particle Imaging. X-rays diffracted from material in the interaction region reflect from a graded-period multilayer-coated mirror to a single photon sensitive X-ray CCD while the direct beam passes through a hole in the center of the mirror. For these experiments, FLASH was operated in multibunch ultrashort pulse mode[1] to increase the rate of particle interception. Pulse bunches were delivered at 5 Hz, and each bunch consisted of 27 X-ray pulses separated by 10 μs. Each pulse was transform limited and typically dominated by a single mode, that is, it had almost complete transverse and longitudinal coherence. This high degree of coherence is a requirement for high-resolution imaging and results in the ability to utilize essentially the entire output of the source for our experiments. The mean photon wavelength was 13.5 nm, the average pulse energy was about 20 μJ, equivalent to about 1.4×10^{12} photons, and the pulse duration was 15 ± 5 fs.

The diffraction pattern recorded by a typical CCD readout when the FEL intercepts a particle is shown in Figure 4A. The strong near vertical and horizontal lines that pass through the center of the pattern are caused by the 200 μm square window aperture (Figure 1, (ii)). This aperture is used to block scattered light from the ellipsoidal mirror that would otherwise add noise to the diffraction pattern. We find that a square aperture produces secondary scattering that is localized in the diffraction pattern and which can be easily filtered from the pattern, whereas a circular aperture distributes secondary scattering across the entire pattern. The dark area on the left of the pattern is a shadow due to the mass spectrometer and the vertical line on the right of the pattern is due to a column defect in the CCD.

This diffraction pattern exhibits the characteristic Airy rings of a spherical particle, indicating that a spherical residue particle is created as the solvent evaporates from the electrospray droplet and the sucrose encapsulates the DNA. The particle diameter (248 ± 10 nm) was determined by fitting the radial average of the signal intensity to Mie theory (Figure 4C). The strategy of encasing material in sucrose has the potential to be refined to create molecular tampers predicted to delay the onset of damage to biomolecules during intense single pulse X-ray exposures.[31]

Several diffraction patterns indicative of two particles being intercepted by a single FEL pulse simultaneously were also captured unexpectedly (Figure 4B). The diffraction pattern shows fringes due to interference between the scattered waves from two particles. This coherent addition would not be present if two particles are hit by two different pulses. Mass spectrometer data collected for each individual FEL pulse during the CCD acquisition verified that only a single particle interception event occurred, producing the mass spectrum in Figure 3C. The well-defined Airy ring pattern in Figure 4C suggests that the two particles hit by the same pulse are of similar diameter, calculated to be 330

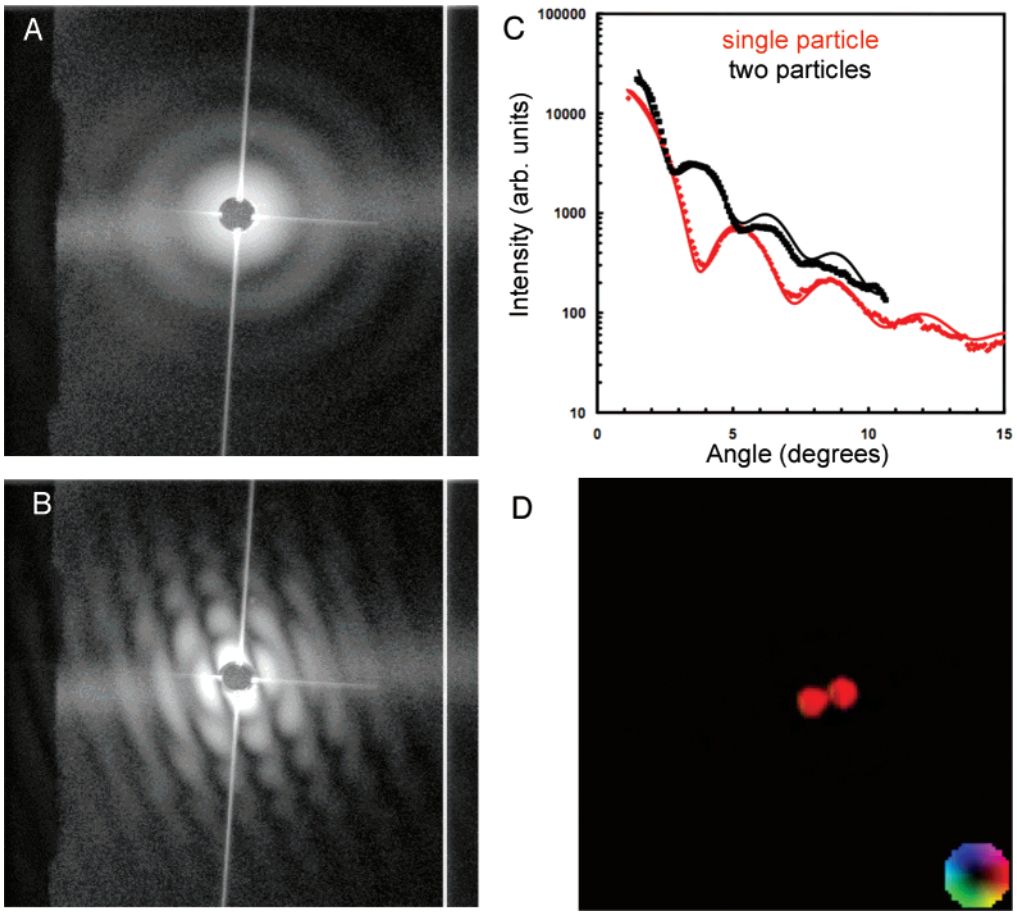

Figure 4. FLASH X-ray coherent diffraction patterns of (A) a single particle and (B) two particles. The intensity is shown on a logarithmic gray scale with black denoting 1 photon/pixel and white denoting 16 500 photons/pixel. Each diffraction pattern is integrated over 243 FEL pulses, one of which intercepted the particles. The entire pattern as detected by the CCD is shown. (C) Radial averages of the angle-resolved signal intensity for the single particle from panel A and the two particles from panel B. The markers are experimental data and the solid lines are calculated with Mie theory, which predicts diameters of 248 ± 10 and 330 ± 20 nm (assuming identical size for the pair) respectively. (D) The X-ray image reconstructed from data in panel B shows that the two particles, each ∼325 nm in diameter, are in contact. Pixel size in the reconstruction is 30.3 nm and the hue denotes the phase of the solution as in the color wheel.

± 20 nm (Figure 4C). The deviation from the Mie theory is attributed to the low signal-to-noise ratio of the diffraction pattern at high angles and the assumption that both particles are of identical diameter. The two minima in the central ring suggest that the distance between the balls in the direction transverse to the beam is the same as their size, that is, the two particles are in contact and constitute a single dimer particle (see Supporting Information). Such a particle could have been created through agglomeration during transport or from two DNA complexes being present in a larger droplet.

Real-space images of nanoscale objects can be obtained from single pulse coherent diffraction patterns using iterative projection algorithms for phase retrieval.[5,7] A reconstructed image of the two-particle pattern reveals that the two particles were in contact, forming a dimer (Figure 4D). The resolution of this image is 40 nm. Each particle was 325 nm in diameter, corresponding to the Mie calculated diameter. This is the first image of a substrate-free individual nanoparticle reconstructed from a diffraction pattern created by a single FEL pulse and represents the first step toward imaging of single biomolecules using future X-ray FELs.

Single Particle Image Acquisition Rate. Over the length of a 2.5 h experiment, a total of 105 particle diffraction patterns were recorded. The average rate was 0.012 particle diffraction patterns collected per second or approximately 1 per minute (Figure 5A, solid square). The expected rate of image collection for this single particle diffractive-imaging technique can be calculated using a modification of an equation derived by Kane et al.[32, 33] for determining aerosol mass spectrometry hit rates (HR)

$$\mathrm{HR} = nVTf\left(\frac{r_\mathrm{L}^2 h}{r_\mathrm{P}^2 v}\right) \quad (1)$$

where n is the aerosol number density, V is the volume flow of aerosol through the inlet, T is the inlet transmission efficiency, h is the X-ray laser beam height (width along the particle beam axis), v is the particle velocity, and r_L and r_P are the radius of the FEL pulse and the particle beam, respectively. The fixed repetition rate, f, of FLASH and the random arrival of particles transmitted through the aerodynamic lens results in hits occurring only when there is

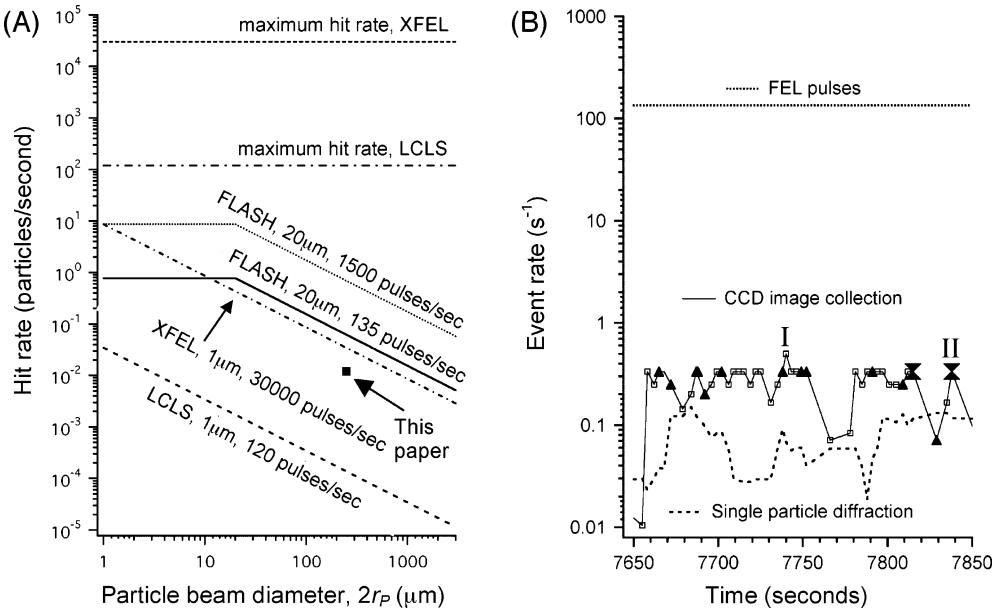

Figure 5. (A) Predicted hit rates at FLASH, XFEL, and LCLS of nanoparticles, electrosprayed to an aerosol concentration of 3×10^4 particles/cm^3, for varying particle beam diameters. The maximum hit rate is equal to the maximum number of pulses per second from the FEL. Annotation denotes X-ray source, FEL beam diameter, and number of pulses delivered per second. The filled square is the average hit rate measured at FLASH during a 2.5 h experiment with 135 FEL pulses/second. (B) Comparison of the rates of FEL pulse (and mass spectrometer acquisition), CCD image acquisition, and single particle diffraction events over a 200 s period of a single particle diffractive imaging experiment. Markers on CCD line: open square = no particle hit, triangle = single particle hit, and double triangle = dimer particle hit. Diffraction patterns collected at CCD readouts I and II are shown in Figure 4.

coincidental overlap of individual particles with the pulsed laser.

Encapsulated DNA nanoparticles were prepared as an aerosol with a concentration of $n = 3 \times 10^4$ particles/cm^3, were sampled by the aerodynamic lens inlet at a rate of $V = 14.33$ cm^3/second, and traveled through the interaction region at $v = 150$ m/s. FEL pulses were delivered at $f = 135$ pulses/second. The interaction volume (Figure 1, point (iii)) is defined by the particle beam diameter ($2r_P = 250$ μm) and the FEL focus ($2r_L = 20$ μm in diameter). Using these parameters, eq 1 predicts a hit rate of 0.06 particles/second, assuming a transmission efficiency of $T = 10\%$ and setting h equal to the particle beam diameter (Figure 5A). The average hit rate (0.07 particles/second) over a 200 s period of our experiment agreed with the predicted hit rate (Figure 5B). The discrepancy between the predicted and measured value over the longer experiment is in part due to steering of the particle beam and down time when changing between pure sucrose and sucrose/DNA samples. We note that the hit rate increases linearly with laser repetition rate, so without modification of our experimental apparatus the hit rate will improve as the FEL pulse rate increases: FLASH has recently been operated at 700 pulses/second with design specifications of over 1500 pulses/second,[2] giving an immediate factor of between 5 and 11 increase in hit rate.

Discussion. Experiments at future hard-X-ray FELs, such as the Linac Coherent Light Source (LCLS) and the European X-ray laser (XFEL), are predicted to enable the determination of three-dimensional (3D) biomolecular structure at near-atomic resolution without crystallization. Such an experiment is anticipated to require acquisition of a large number of images to take advantage of numerical alignment and averaging procedures, thus maximizing the hit rate achievable by single particle imaging is critical to reduce the data acquisition time. Further exacerbating the challenge is that the X-ray beam must be focused down to much smaller spot sizes, typically below 1 μm, to increase the incident intensity and ensure adequate signal at the higher photon momentum transfers (higher resolutions) that the shorter wavelength affords. This will immediately decrease the efficiency of the apparatus demonstrated here by a factor of 400 or more based on the 20 μm diameter FEL beam at FLASH.

FEL laser repetition rate is another critical factor. At the European XFEL, the inefficiencies due to FEL beam size will be made up by the increased FEL pulse rate of up to 30 000 pulses/second. For a source aerosol concentration of 3×10^4 particles/cm^3, this results in an expected hit rate that is only half of that measured at FLASH during the experiments reported in this letter. Hit rates at LCLS may be significantly lower because the planned pulse rate is 120 pulses/second. We summarize the potential hit rates at FLASH and future FEL facilities in Figure 5A, considering only FEL machine parameters and assuming no further improvements in aerodynamic focusing or aerosol density. This is therefore a pessimistic estimate assuming no further sample-handling development.

Image acquisition rates will be improved in a number of ways independent of the X-ray source used. For example, improved particle beam focusing to match the submicron FEL beam size may be possible through developments in the aerodynamic lens stack itself. If the exit nozzle of the aerodynamic lens stack is positioned in closer proximity to

the interaction region, the effect of the divergence angle (currently 0.5−3 degrees) of the particle beam imparted by gas expansion will be reduced. It may also be possible to increase the particle density sampled by the aerosol-handling system using multinozzle electrospray or droplet sources.[34,35]

A key advantage of using aerodynamic focusing for single particle X-ray diffractive imaging is that it is a leak in the vacuum chamber that continuously samples from atmospheric pressure (at a rate of 14.33 $cm^3\ s^{-1}$ for the current design). Thus any aerosol existing near the inlet is passively sampled. This enables us to utilize the advantages of well-characterized atmospheric aerosol sources such as electrospray for preparing samples to be imaged. Many other atmospheric pressure aerosolization methods, including flames, atomizers, and lasers, can also be used. All of these aerosol sources can be interchanged instantaneously or operated simultaneously. Many of these aerosol sources can generate particle concentrations equivalent to or greater than the 3×10^4 particles/cm^3 used here. Each type of source generates particles and size distributions with unique characteristics that make them more or less applicable to the nanoscale biomaterials we studied by electrospray. For example, aerosol sources used in atomic cluster research often operate at concentrations of 10^{10} clusters/cm^3 and will certainly be a useful source for single particle X-ray diffractive imaging of core−shell structured atomic clusters. However, they are currently not suitable for biomolecule imaging. To put these aerosol concentrations into a real-world perspective, measurements of the aerosol concentration generated by automobiles near highways show a total of 10^4-10^6 particles/cm^3,[36] suggesting it may even be possible to image environmental particles.

Another advantage of the aerodynamic lens interface is its ability to continuously operate for many hours without clogging, a crucial characteristic for successful utilization of precious X-ray FEL beam time. The key limitation of this method is the current inability to time the arrival of particles with the FEL pulses. Single particle sources designed to deliver proteins in synchronization with the X-ray pulses are also being developed[37] and if successful may overcome the inefficiency of operation in free-fire mode. It is anticipated that continued development of single particle sources of all types will increase the number of accessible sample types and raise the achievable hit rate to the maximum levels available for both LCLS and XFEL. Detectors designed to accommodate single particle diffraction data acquisition at such high rates are in development.

The ultimate goal for single molecule X-ray imaging is the delivery of a sufficient number of identical molecules to enable 3D reconstruction. Any diffraction patterns of nonidentical molecules collected will reduce the effective hit rate and increase the complexity of classifying images of molecules in different orientations. Future experiments will make use of particle size selection technology such as differential mobility methods.[20] This approach can be used to remove contaminants such as residue particles or to select molecular conformations, potentially reducing the complexity of classifying diffraction patterns. Also note that the thickness of the sucrose coatings, which in our experiments had a broad distribution, can currently be controlled to less than 1 nm.[29]

The resolution obtained in single pulse X-ray imaging experiments is limited in part by the onset of damage in the sample due to the intense X-ray pulse. Depending on the pulse duration, the resolution limit may be 0.5 nm for hard-X-ray FEL pulses or even less with encapsulated particles.[31] For the pulse fluences and wavelength of these experiments, calculations show that the diffraction pattern formed by the pulse would be essentially the same as the undamaged case and that any expansion of the particle would certainly be much less than the resolution length of 40 nm.[38] Furthermore, diffractive imaging of well-characterized nanostructured objects at FLASH at 32 nm wavelength has shown no measurable damage.[5] In the experiments reported here, we are not able to probe the extent of damage in the sample due to unknown shape and size characteristics of the individual sucrose-encapsulated DNA particles imaged during a specific pulse. Future work investigating the onset of damage in particles in free flight will utilize size-monodisperse spherical nanoparticles that have been diameter selected by differential mobility methods[20] and sampled directly into the aerodynamic lens stack. This approach will be an extension of our method for measuring X-ray pulse-induced damage at femtosecond time resolutions with size-selected spherical nanoparticles deposited onto silicon nitride membranes.[4]

Our results unequivocally show the feasibility of single-particle X-ray diffractive imaging using FELs. It is expected that future X-ray FEL facilities will enable nanometer to atomic scale resolution imaging of noncrystalline nanoscale materials, such as large biomolecules, viruses or cells, inorganic particles, and environmental particles. Single particle X-ray diffractive imaging will provide new capabilities for following the dynamics of materials at the atomic time and length scales, potentially resulting in significant advances in nanotechnology development and structural biology.

Acknowledgment. Special thanks are due to the scientific and technical staff of the FLASH at DESY, Hamburg, in particular to R. Treusch, J. Schneider, S. Dusterer, T. Tschentscher, J. Feldhaus, R. L. Johnson, U. Hahn, T. Nuñez, K. Tiedtke, S. Toleikis, E. L. Saldin, E. A. Schneidmiller, and M. V. Yurkov. We are grateful to our collaborators in T. Möller's group at Technische Universitat Berlin for accommodating our experiment in their vacuum chamber. We also thank D. Shapiro, T. McCarville, F. Weber, and M. Haro for technical help with these experiments. This work was supported by the following agencies: The U.S. Department of Energy by Lawrence Livermore National Laboratory in part under Contract W-7405-Eng-48 and in part under Contract DE-AC52-07NA27344, Lawrence Livermore National Laboratory (the project 05-SI-003 from the Laboratory Directed Research and Development Program of LLNL); The National Science Foundation Center for Biophotonics, University of California, Davis, under Cooperative Agreement PHY 0120999; The National Center for Electron Microscopy and the Advanced Light Source, Lawrence Berkeley Lab,

under DOE Contract DE-AC02-05CH11231; the DOE Office of Science to the Stanford Linear Accelerator Center; the European Union (TUIXS); The Swedish Research Council; The Swedish Foundation for International Cooperation in Research and Higher Education; The Swedish Foundation for Strategic Research; The Sven and Lilly Lawskis Fund (Doctoral Fellowship to MMS) and the Natural Sciences and Engineering Research Council of Canada (NSERC Postdoctoral Fellowship to M.J.B).

Supporting Information Available: Experimental details and Fourier transform images. This material is available free of charge via the Internet at http://pubs.acs.org.

References

(1) Ayvazyan, V.; Baboi, N.; Bahr, J.; Balandin, V.; Beutner, B.; et al. *Eur. J. Phys. D* **2006**, *37*, 297−303.
(2) Ackermann, W.; Asova, G.; Ayvazyan, V.; Azima, A.; Baboi, N.; et al. *Nat. Photonics* **2007**, *1* (6), 336−342.
(3) Gaffney, K. J.; Chapman, H. N. *Science* **2007**, *316* (5830), 1444−1448.
(4) Chapman, H. N.; Hau-Riege, S. P.; Bogan, M. J.; Bajt, S.; Barty, A.; et al. *Nature* **2007**, *448* (9), 676−679.
(5) Chapman, H. N.; Barty, A.; Bogan, M. J.; Boutet, S.; Frank, M.; et al. *Nat. Phys.* **2006**, *2* (12), 839−843.
(6) Fienup, J. R. *Appl. Opt.* **1982**, *21*, 2758−2769.
(7) Marchesini, S. *Rev. Sci. Instrum.* **2007**, *78* (4), 011301.
(8) Neutze, R.; Wouts, R.; van der Spoel, D.; Weckert, E.; Hajdu, J. *Nature* **2000**, *406*, 752−757.
(9) Huldt, G.; Szoke, A.; Hajdu, J. *J. Struct. Biol.* **2003**, *144*, 219−227.
(10) Spence, J. C. H.; Doak, B. *Phys. Rev. Lett.* **2004**, *92*, 198102.
(11) Piseri, P.; Tafreshi, H. V.; Milani, P. *Curr. Opin. Solid State Mater. Sci.* **2004**, *8* (3−4), 195−202.
(12) Carbone, R.; Giorgetti, L.; Zanardi, A.; Marangi, I.; Chierici, E.; et al. *Biomaterials* **2007**, *28* (13), 2244−2253.
(13) Noble, C. A.; Prather, K. A. *Mass Spectrom. Rev.* **2000**, *19*, 248−274.
(14) Wilson, K. R.; Peterka, D. S.; Jimenez-Cruz, M.; Leone, S. R.; Ahmed, M. *Phys. Chem. Chem. Phys.* **2006**, *8* (16), 1884−1890.
(15) Shu, J.; Wilson, K.; Ahmed, M.; Leone, S. R. *J. Chem. Phys.* **2006**, *124*, 034707.
(16) Liu, P.; Ziemann, P. J.; Kittleson, D. B.; McMurry, P. H. *Aerosol Sci. Technol.* **1995**, *22*, 314−324.
(17) Liu, P.; Ziemann, P. J.; Kittleson, D. B.; McMurry, P. H. *Aerosol Sci. Technol.* **1995**, *22*, 293−313.
(18) Wexler, A. S.; Johnston, M. V. Real-time single-particle analysis. In *Aerosol Measurement*; Baron, P. A., Willeke, K., eds.; John Wiley & Sons: Hoboken, NJ, 2005; pp 365−386.
(19) Chen, D. R.; Pui, D. Y. H.; Kaufman, S. L. *J. Aerosol Sci.* **1995**, *26* (6), 963−977.
(20) Bogan, M. J.; Benner, W. H.; Hau-Riege, S. P.; Chapman, H. N.; Frank, M. *J. Aerosol Sci.* **2007**, *38* (11), 1119−1128.
(21) O'Shea, J. N.; Taylor, J. B.; Swarbrick, J. C.; Magnano, G.; Mayor, L. C.; et al. *Nanotechnology* **2007**, *18* (3), 035707.
(22) Bacher, G.; Szymanski, W. W.; Kaufman, S. L.; Zollner, P.; Blaas, D.; et al. *J. Mass Spectrom.* **2001**, *36*, 1038−1052.
(23) Hogan, C. J. J.; Kettleson, E. M.; Ramaswami, B.; Chen, D. R.; Biswas, P. *Anal. Chem.* **2006**, *78* (3), 844−852.
(24) Bothner, B.; Siuzdak, G. *ChemBioChem* **2004**, *5*, 258−260.
(25) Tito, M. A.; Tars, K.; Valegard, K.; Hajdu, J.; Robinson, C. V. *J. Am. Chem. Soc.* **2000**, *122* (14), 3550−3551.
(26) Blades, A. T.; Ikonomou, M. G.; Kebarle, P. *Anal. Chem.* **1991**, *63* (19), 2109−2114.
(27) Rothemund, P. W. K. *Nature* **2006**, *440*, 297−302.
(28) Hau-Riege, S. P.; Szoke, H.; Chapman, H. N.; Szoke, A.; Marchesini, S.; et al. *Acta Crystallogr., Sect. A* **2004**, *60* (4), 294−305.
(29) Kaufman, S. L. *Anal. Chim. Acta* **2000**, *406* (1), 3−10.
(30) Taylor, V. F.; March, R. E.; Longerich, H. P.; Stadey, C. J. *Int. J. Mass Spectrom.* **2005**, *243* (1), 71−84.
(31) Hau-Riege, S. P.; London, R. A.; Chapman, H. N.; Szoke, A.; Timneanu, N. *Phys. Rev. Lett.* **2007**, *98*, 198302.
(32) Kane, D. B.; Johnston, M. V. *Environ. Sci. Technol.* **2000**, *34*, 4887−4893.
(33) Kane, D. B.; Oktem, B.; Johnston, M. V. *Aerosol Sci. Technol.* **2001**, *34* (6), 520−527.
(34) Deng, W.; Klemic, J. F.; Li, X.; Reed, M. A.; Gomez, A. *J. Aerosol Sci.* **2006**, *37*, 696−714.
(35) Bocanegra, R.; Galan, D.; Marquez, M.; Loscertales, I. G.; Barrero, A. *J. Aerosol Sci.* **2005**, *36*, 1387−1399.
(36) Kittelson, D. B.; Watts, W. F.; Johnson, J. P.; Remerowki, M. L.; Ische, E. E.; et al. *Inhalation Toxicol.* **2004**, *16* (11 supp 1), 31−39.
(37) Weierstall, U.; Doak, R. B.; Spence, J. C. H.; Starodub, D.; Shapiro, D.; et al. *Exp. Fluids*, in press.
(38) Hau-Riege, S. P.; London, R. A.; Bergh, M.; Chapman, H. N. *Phys. Rev. E* **2007**, *76*, 046403.

NL072728K